Effect of β-Nucleating Agents on Crystallization and Melting Behavior of Isotactic Polypropylene

Wenchang Xiao, Peiyi Wu, Jiachun Feng

Key Laboratory of Molecular Engineering of Polymers of Ministry of Education, Department of Macromolecular Science, Fudan University, Shanghai 200433, People's Republic of China

Received 10 November 2007; accepted 2 January 2008
DOI 10.1002/app.27997
Published online 5 March 2008 in Wiley InterScience (www.interscience.wiley.com).

ABSTRACT: Two kinds of β-nucleating agents, named a rare earth complex (WBG) and a *N*,*N*′-dicyclohexylterephthalamide (TMB5), were introduced into isotactic polypropylene (iPP), and their effect on crystallization and melting behavior of iPP was comparatively investigated. Wide angle X-ray diffraction measurements revealed that both the two additives were highly effective in inducing β modification. At their respective optimum concentrations of 0.08 wt % for WBG and 0.06 wt % for TMB5, the relative amount of β-form calculated by Turner-Jones equation both exceeds 92%. However, the isothermal crystallization kinetics investigated by differential scanning calorimetry demonstrated that WBG had more pronounced effect than TMB5 in accelerating the overall crystallization rate. The Lauritzen–Hoffman theory analysis also revealed that WBG was more effective not only in increasing the nucleus number but also in accelerating the growth rate of crystallization. After completing isothermal crystallization process, the subsequent melting behavior examination suggested that the addition of WBG expanded the upper limit temperature of forming β modification, and therefore was more effective in delaying the β-α transformation than TMB5. © 2008 Wiley Periodicals, Inc. J Appl Polym Sci 108: 3370–3379, 2008

Key words: isotactic polypropylene; crystallization; polymorphism; nucleating agent; β-α transformation

INTRODUCTION

Isotactic polypropylene (iPP) is a widely used and versatile commodity polymer with numerous advantages, such as low density, ease of processing, recyclability, and excellent mechanical performances. As one of the most important polymorphic materials, iPP exhibits several polymorphs (α, β, γ, etc.).[1] The intrinsic architecture and extrinsic parameters affect mostly through their influence on crystallization behavior and morphological features, which are probably the most important factors affecting the final physical properties. Therefore, controlling the growth rate and tailoring the proportion of different polymorphs is extremely important for iPP applications.

The particular interest in β-form isotactic polypropylene (β-iPP) arises from the fact that, as a result of its different spherulitic architecture, the β-form has some unique characteristics such as a lower melting temperature and improved mechanical properties (especially the higher impact strength) in comparison with the more common α-form.[2–8] However, the β-form is thermodynamically metastable and difficult to obtain under normal processing conditions. A higher proportion of the β-form can be achieved only by melt crystallization with the aid of certain heterogeneous nucleating agents,[2–12] by directional crystallization in certain temperature gradients,[13,14] or from melts subject to shear.[15,16] Among these the addition of so-called β-nucleating agents is an effective and practical method not only to obtain or increase the β-form in iPP, but also to shorten the crystallization time so as to expedite the cycle time of production.

Compared with diverse α-nucleating agents, β-nucleating agents are more selective, and there are fewer compounds used as β-nucleating agents. Until now, only three classes of compounds have been mainly used as β-nucleating agents[17]: the first class is a minority of aromatic ring compounds, such as γ-quinacridone (Dye Permanent Red E3B) and triphenodithiazine[2]; the second class includes certain group IIA metal salts or their mixtures with some specific dicarboxylic acids, such as calcium salt of imido acids and compounds of calcium stearate and pimelic acid[3,4]; the third class is some substituted aromatic bisamides, mainly includes *N*,*N*′-dicyclohexylterephthalamide and *N*,*N*-dicyclohexyl-2,6-naphthalene dicarboxamide.[5–8] Although several β-nucleating agents have been proposed and patented, the commercial β-nucleating agents are still rather

Correspondence to: J. Feng (jcfeng@fudan.edu.cn).
Contract grant sponsor: National Natural Science Foundation of China; contract grant number: 50673021.
Contract grant sponsor: National Basic Research Program of China; contract grant number: G2005CB623803.
Contract grant sponsor: Natural Science Foundation of Shanghai; contract grant number: 06ZR14007.

limited. Hence, the development of an effective, cheap, and accessible β-nucleating agent remains an essential topic in the composite material research field.

It was found in our previous research that although having low nucleating activity (the relative amount of β-form was no more than 25%), some mixtures consisting of rare earth compounds and some mineral additives could induce β-form formation.[18,19] We surmised that the true β-iPP nucleating agent in these systems might be some binuclear complexes of calcium and rare earth elements with some ligands. Based on this idea, we synthesized a series of heteronuclear dimetal complexes of lanthanum and calcium with some specific ligands, which have been industrially prepared and applied as a commercial β-nucleating agent production.

In this article, a rare earth based β-nucleating agent (WBG) and an aromatic dicarboxamide compound β-nucleating agent (TMB5) were comparatively investigated on their nucleating activities and its effect on isothermal crystallization, as well as the subsequent melting behavior of iPP. TMB5 is chosen as a comparison because of the fact that the major component of TMB5, *N*,*N*′-dicyclohexylterephthalamide, is a widely used β nucleating agent and has been intensively studied.[5–8,20]

EXPERIMENTAL

Materials

The iPP employed in this work was F401, a product of the Yangzi Petrochemical, SINOPEC (Nanjing, China); it had a melt flow rate (MFR) of 2.5 g/10 min (230°C, 2.160 kg), a density of 0.91 g/mL and a tacticity of 96.5%. A small amount of antioxidant (Irganox 1010 and 168) existed in the as-received iPP; therefore, no additional antioxidant was used. Two β-nucleating agents were used in this work. The rare earth β-nucleating agent, WBG, was a heteronuclear dimetal complex of lanthanum and calcium with some specific ligands. It was kindly supplied by Guangdong Winner Functional Materials Co. (Foshan, Guangdong Province, China). The WBG has a general formula of $Ca_xLa_{1-x}(LIG1)_m(LIG2)_n$, where x and $1 - x$ is the proportion of Ca^{2+} and La^{3+} ion in the complex, while LIG1 and LIG2 are respectively a dicarboxylic acid and amide-type ligand with coordination numbers of m and n. The TMB5 β-nucleating agent with a chemical component of *N*,*N*′-dicyclohexylterephthalamide was supplied by Shanxi Institute of Chemical Industry (Taiyuan City, China).

Sample preparation and characterization

The samples were prepared with a two-step procedure. First, the β-nucleating agents were mixed with the iPP pellets on a PL-651 Brabender Mixer (Brabender, Germany) at 170°C. The roller speed was 45 rpm and the mixing time in the mixing chamber was 7 min. It is reported that β-form grows faster than α-form in a large central part of the crystallization range (100–140°C), and the most favorable temperature for the growth of β-form is at about 123°C.[7,21] To gain samples with high level of β-form, the mixture was subsequently molded into 0.4-mm-thick sheets at 190°C under a pressure of 15 MPa for 5 min and then transferred to another press machine and maintained at 120°C under a pressure of 5 MPa for an another 30 min before being naturally cooled to room temperature. To determine the optimum loadings of nucleating agents, we evaluated the amount of β-form as a function of the nucleating agent concentration by wide angle X-ray diffraction (XRD) measurements. It was found that the base resin may be fully nucleated at concentrations of 0.08 wt % of WBG and 0.06 wt % of TMB5. Therefore, the iPP modified by 0.08 and 0.06 wt % of WBG and TMB5 were prepared and denoted as iPP/WBG and iPP/TMB5, respectively. Also, a pure iPP sample was prepared with an identical mixing and molding schedule was used as a control (denoted as virgin iPP).

All the specimens for XRD and differential scanning calorimetry (DSC) measurements were cut from 0.4-mm-thick sheets. XRD measurements were performed using a PANalytical X'pert diffractometer (PANalytical, Netherlands) in a reflection mode using Ni-filtered CuKα radiation (λ = 0.154 nm) under a voltage of 40 kV and a current of 40 mA. Radial scans of intensity versus diffraction angle 2θ were recorded in the region of 5–30°. After the usual correction, the X-ray curves were resolved into contributions of crystalline peaks and amorphous peaks. The overall degree of crystallinity (X_c) of each sample was determined from the peak areas in the region of 10–30°, and the relative proportion of the β-form in the crystalline part was calculated by the widely accepted empirical equation of Turner-Jones et al.[22]

DSC measurements were carried out using a Q-100 thermal analysis system (TA Instruments Inc. DE) with a nitrogen purge of 50 mL/s. The temperature calibration was performed using standard indium. A range of 6–9 mg of each sample was first heated to 200°C at a scanning rate of 10°C/min and maintained at that temperature for 5 min to diminish the influence of the previous thermal and mechanical history; they were then cooled to 40°C at a standard cooling rate of 10°C/min to determine the temperature at the onset of the apparent crystallization, $T_{c\text{-onset}}$. Also, after the elimination of the thermal and mechanical history, samples were then cooled rapidly to the predetermined crystallization temperature (T_c) and maintained until the completion of crystallization. The given T_c for virgin iPP were 126,

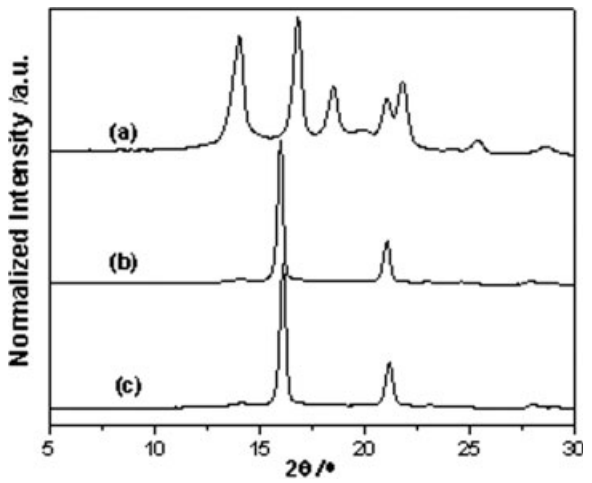

Figure 1 XRD patterns for (a) virgin iPP, (b) iPP/WBG, and (c) iPP/TMB5, respectively.

128, 130, 132, and 134°C, respectively, while these temperatures for both iPP/WBG and iPP/TMB5 were 134, 136, 138, 140, 141, 142, 143, and 144°C. Subsequently, the samples after isothermal crystallization were reheated from 40 to 200°C at a scanning rate of 10°C/min and the melting process was recorded.

RESULTS AND DISCUSSION

Effectiveness of β-nucleating agents

Figure 1(a) shows the XRD pattern of virgin iPP. Within the given range of reflection angles, there are five local maxima at 2θ values of approximately 14.0, 16.8, 18.6, 21.2, and 21.8°, corresponding to the (110), (040), (130), and overlapping (131) and (111) reflections, which are characteristic peaks of monoclinic α-form. However, as shown in Figure 1(b,c) of the XRD patterns for iPP/WBG and iPP/TMB5, almost no features associated with α-form, but only two peaks stand for the β-crystalline phase at 2θ = 16.0° representing the (300) plane and that at 2θ = 21.0° accounting the (301) plane, is observed. These changes clearly indicate that dominant modification in the virgin iPP sample is α-form, while that in iPP/WBG and iPP/TMB5 is β-form.

The relative proportion of the β-form in the crystalline part, k_β, is determined with the Turner-Jones equation:[22]

$$k_\beta = \frac{H(\beta)}{H(\beta) + H(\alpha 1) + H(\alpha 2) + H(\alpha 3)} \times 100\% \quad (1)$$

where $H(\alpha 1)$, $H(\alpha 2)$, and $H(\alpha 3)$ are the intensities of the three α-diffraction peaks (110), (040), and (130), respectively, and $H(\beta)$ is the intensity of the strong single β-peak (300) at 2θ = 16.0°.

The k_β value is about 92 and 93% for iPP/WBG and iPP/TMB5, and 0% for virgin iPP, which reveals that both WBG and TMB5 induce almost pure β-form and act as highly efficient β-nucleating agents. The comparable k_β values for the two nucleated samples suggest that no substantial variation exists between the two additives.

Figure 2 shows the DSC thermograms of various samples recorded during the first melting scan. It is apparent that these traces exhibit two endothermic melting peaks. The multiple endotherms may be assigned to the existence of two different crystalline forms. The endotherm at lower peak temperature of ~ 154°C could be associated with the melting of the β-form, while another endotherm approximately located at 167°C is characteristic for the melting of the α-form. As shown in Figure 2(a), the melting trace of virgin iPP mainly exhibits the melting of α-form. In contrast, the β-nucleated samples with WBG or TMB5 crystallized mostly in β-form, as indicated by the absolutely dominant β-melting peaks in Figure 2(b,c).

DSC is often used in laboratory routine as an alternative to XRD to estimate the relative content of the β-form in a sample.[23] The relative content of β-form estimated by DSC melting curves may be defined as ϕ_β and calculated from the following equation:

$$\phi_\beta = \frac{X_\beta}{X_\alpha + X_\beta} \times 100\% \quad (2)$$

where X_α and X_β are the crystallinity of the α- and β-form, respectively, and could be calculated separately according to

$$X_i = \frac{\Delta H_i}{\Delta H_i^0} \times 100 \quad (3)$$

where ΔH_i is the calibrated specific fusion heat of either the α- or the β-form and ΔH_i^0 is the standard

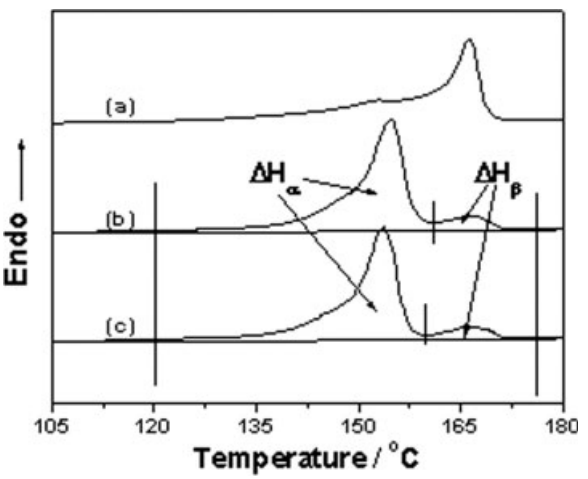

Figure 2 DSC melting traces with a standard heating rate (10°C/min) for (a) virgin iPP, (b) iPP/WBG, and (c) iPP/TMB5, respectively.

fusion heat of either α- or β-form, 177 J/g for α-form and 168.5 J/g for β-form.[24] Because of the coexistence of α- and β-forms, the samples exhibited both an α-fusion peak and a β-fusion peak on DSC curves, which overlapped partially. The total fusion heat was estimated by integrating the DSC thermogram from 120 to 178°C. A vertical line was drawn through the minimum between the α-fusion peak and β-fusion peaks, and the total fusion heat was divided into β-component and α- component. The specific fusion heats for α- and β-forms were determined according to the calibration method reported in the Refs. 25 and 26. The ϕ_β values for sample iPP/WBG and iPP/TMB5 both exceed 90%. These results further revealed that almost pure β-form were present in samples nucleated with these nucleating agents. Thus, the calorimetric results accord very well with the XRD structure determinations.

After the elimination of the thermal history, each sample was cooled to 40°C to determine the temperature at the onset of the apparent crystallization, $T_{c\text{-onset}}$, with a standard cooling rate of 10°C/min. In comparison with the $T_{c\text{-onset}}$ value of 119.9°C for virgin iPP, the values for iPP/TMB5 and iPP/WBG are 123.5°C and 130.4°C, respectively. In industrial production, an increase in the $T_{c\text{-onset}}$ is usually used to judge the effectiveness of nucleating agents.[27–29] A larger increase on $T_{c\text{-onset}}$ represents a higher efficiency of the heterogeneous nucleation, which has obvious advantages for extrusion and injection molding processes. From this point of view, the considerable improved $T_{c\text{-onset}}$ of iPP/WBG system suggests that WBG is a more efficient nucleating agent.

Isothermal crystallization and subsequent melting behavior

The isothermal crystallization kinetics of virgin iPP and β-nucleated iPPs can be analyzed by evaluating the degree of crystalline conversion as a function of time at a constant crystallization temperature (T_c). The relative crystallinity, X_t, is calculated by integration of the exothermal peaks from the following equation:

$$X_t = \frac{X_t(t)}{X_t(\infty)} = \int_0^t \left(\frac{dH}{dt}\right) dt \Big/ \int_0^\infty \left(\frac{dH}{dt}\right) dt \qquad (4)$$

where (dH/dt) is the rate of heat evolution, $X_t(t)$ and $X_t(\infty)$ represent the absolute crystallinity at time t and at the termination of the crystallization process, respectively. Figure 3 shows the curves of relative crystallinity X_t versus crystallization time t for (a) virgin iPP, (b) iPP/WBG, and (c) iPP/TMB5 at indicated isothermal crystallization temperatures, from which the effect of T_c on the crystallization rate could be clearly observed. As shown in Figure 3(a), at T_c = 126°C it takes about 9 min for virgin iPP to complete the crystallization, while at T_c = 134°C the value increases to 60 min. The crystallization temperature has a similar influence on the crystallization rate of iPP/WBG and iPP/TMB5, as shown in Figure 3(b,c). During isothermal crystallization, half crystallization time, $t_{1/2}$, corresponding to 50% of the crystal conversion, is frequently used to evaluate the crystallization rate of iPP. The shorter the $t_{1/2}$ is, the faster the crystallization rate. The $t_{1/2}$ values

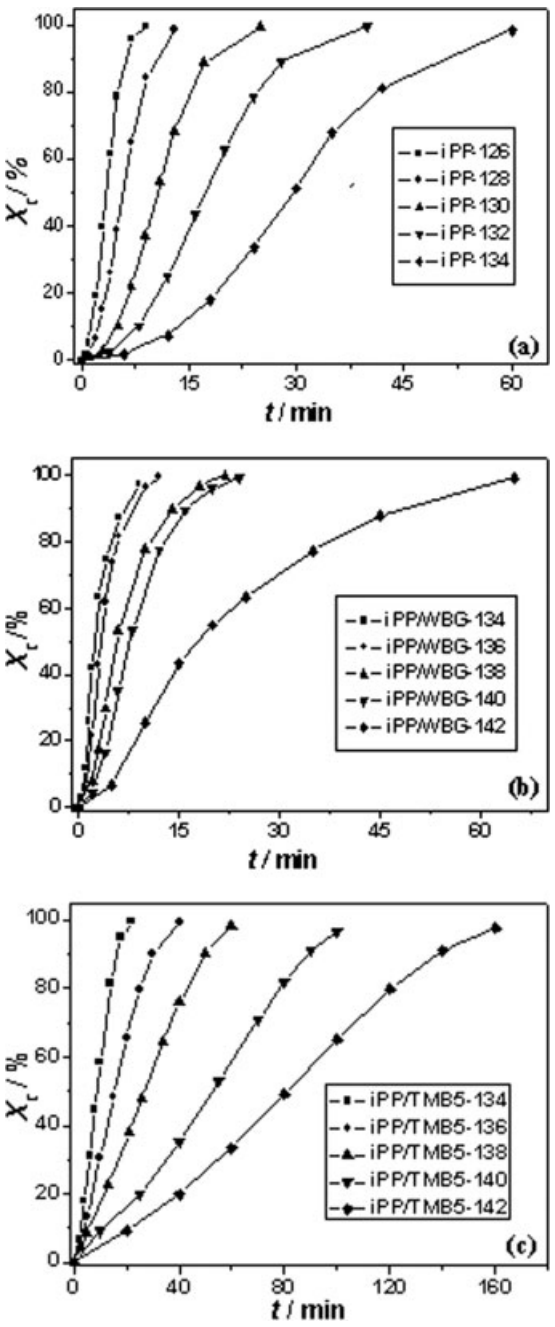

Figure 3 Dependence of the relative crystallinity on crystallization time for (a) virgin iPP, (b) iPP/WBG, and (c) iPP/TMB5, at indicated crystallization temperature.

TABLE I
Isothermal Crystallization Kinetic Data of iPP and Nucleated iPPs

Sample	T_c (°C)	Z_t (min^{-n})	n	$t_{1/2}$[a] (min)	$t_{1/2}$[b] (min)	n (average)	K_g (10^5 K^2)	σ_e (J/m^2)
iPP	126	0.057	2.05	3.5	3.5	2.28	9.97	0.166
	128	0.016	2.16	5.9	5.9			
	130	0.0021	2.45	10.2	10.4			
	132	0.00087	2.35	17.4	17.5			
	134	0.00023	2.37	29.6	29.8			
iPP/WBG	134	0.12	2.19	2.2	2.4	2.05	6.64	0.111
	136	0.061	2.02	3.3	3.2			
	138	0.020	2.03	5.7	5.9			
	140	0.010	2.09	7.6	7.7			
	142	0.0032	1.92	17.9	18.0			
iPP/TMB5	134	0.021	1.62	8.6	8.7	1.62	7.58	0.126
	136	0.013	1.45	15.5	15.5			
	138	0.0052	1.51	26.5	25.5			
	140	0.00080	1.72	52.4	51.1			
	142	0.00028	1.79	81.2	78.7			

[a] Determined from Figure 3.
[b] Calculated from the Avrami equation.

obtained from curves of X_t versus t in Figure 3 are listed in Table I. The increase in the $t_{1/2}$ with increasing of T_c also suggests that higher T_c leads to prolonged crystallization time and decreased crystallization rate.

The dependence of $t_{1/2}$ on crystallization temperature T_c is shown in Figure 4. At identical T_c, for example 134°C, the $t_{1/2}$ is about 30.1, 2.2, and 9.0 min for virgin iPP, iPP/WBG, and iPP/TMB5, respectively. The essential reduced $t_{1/2}$ for nucleated samples reveals that both nucleating agents are efficient in accelerating the crystallization rate of iPP. However, for two β-nucleated iPPs, the $t_{1/2}$ for sample iPP/WBG is much smaller than that for iPP/TMB at the same T_c, especially at a higher crystallization temperature. The $t_{1/2}$ is 9.1 min for sample iPP/WBG and 53.3 min for iPP/TMB at T_c of 140°C, increasing by almost four and six times compared with these values at 134°C, respectively. The dependence of $t_{1/2}$ on T_c is smaller for iPP/WBG than that of iPP/TMB5. In other words, the iPP/TMB5 is more sensitive to T_c increase in declining the crystallization rate. These results reveal that the nucleation effect of WBG is superior to TMB5 at the whole T_c region investigated in this work, especially in the higher crystallization temperature. Wang et al.[30] evaluated the efficiency of a nucleation agent using $t_{1/2}$ and found that when nucleated PPs isothermally crystallized at high temperatures (above 136–137°C), the nucleating agents would lose their efficiency. Kim and coworkers[31] have studied the nucleation effect of a series of sorbitol derivatives on PP crystallization and concluded that the temperature dependence of a nucleating agent might be treated as a characteristic of a given polymer/nucleating agent mixture. Therefore, the different temperature dependences between system iPP/WBG and iPP/TMB5 on the crystallization rate ($t_{1/2}$) may essentially be ascribed to the different characteristics of the two nucleating agents.

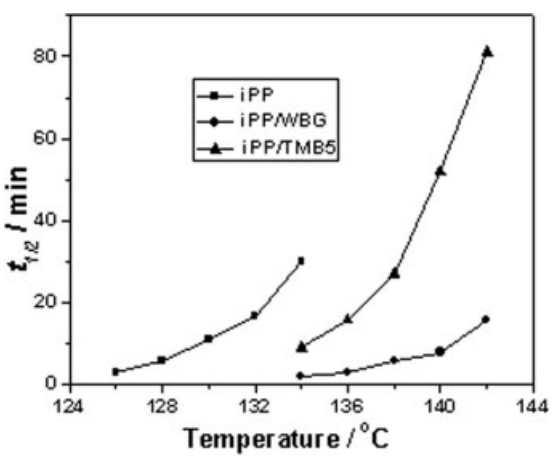

Figure 4 Dependence of the $t_{1/2}$ on crystallization temperature for virgin iPP and β-nucleated iPPs.

As shown in Figure 5(a), at isothermal crystallization temperatures higher than 136°C, the iPP/TMB5 shows an unusual crystallization behavior, and multiple exothermic peaks A and B occur on DSC crystallization traces. The first exothermic peak A becomes more significant with the increase of T_c. However, such double exotherm characteristic is not observed for either iPP/TMB5 at a lower T_c (below 136°C) or iPP/WBG sample at whole T_c region studied in this work (Fig. 5(b)). There is only single crystallization peak on the DSC traces for these samples. To investigate this process more distinctly, a partialy crystallization-melting measurement was performed: after the elimination of the thermal history, the melted samples were cooled rapidly to a given crystallization temperature (for example, 138°C) where

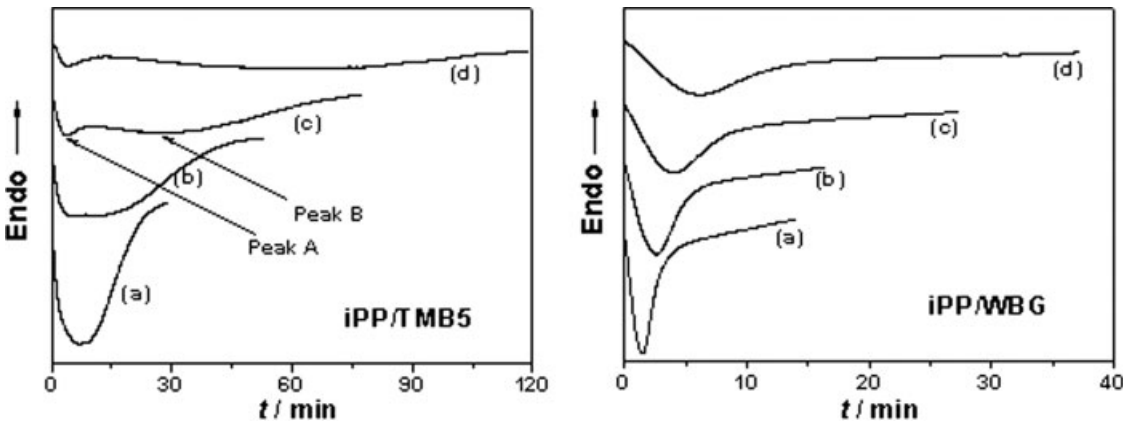

Figure 5 DSC traces of iPP/TMB5 (left) and iPP/WBG (right) isothermally crystallized at (a) 134, (b) 136, (c) 138, and (d) 140°C, respectively.

there exist double exothermic peaks during isothermal crystallization, kept isothermally crystallizing at this temperature for various time t (10, 20, 40, 60, and 80 min), and then heated to 200°C with 10°C/min. The DSC melting traces are shown in Figure 6. It is notable that there is only β-form melting peak present on the melting traces after a short isothermal crystallizition time, for example, 10 min, approximately the time of the first exothermic peak occurrence. However, with increasing crystallization time, the melting peak referring to α-form presents and its intensity also increases as time prolongs. Furthermore, when prolonging the crystallization time, the positions of the melting peaks for either α-form or β-form shifts to higher temperature, which may attribute to the improved crystal perfection due to longer crystallization time. These results demonstrate that β-form growth was preferred in the initial crystallization period, and α-form subsequently occurred and developed with the concomitance of the continually developed β-form. Vychopnová et al.[20] also found such multiple exothermic characteristic when iPP nucleated with a minute amount of NJS β-nucleating agent (*N*,*N*-dicyclohexyl-2,6-naphthalene dicarboxamide) isothermally crystallized at a higher temperature of 140°C. Recently, Menyhard et al.[32] comparatively investigated the nucleating efficiency and selectivity of some different β-nucleating agents. They proved that the efficiency and the selectivity of Ca-suberate and Ca-pimelate are extremely high in a wide concentration range, while NJS is highly efficient but not completely selective. The phenomena of double exothermic peaks on DSC crystallization traces largely depended on the concentration and the type of β-nucleating agent. This is in accord with the observation in the present work. The results shown in Figures 5 and 6 suggest that the TMB5 that has a similar chemical structue as NJS is less selective than WBG, at least under high crystallization temperatures.

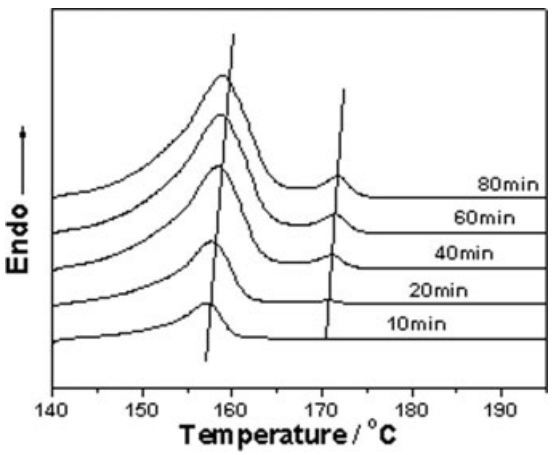

Figure 6 DSC melting traces of sample iPP/TMB5 after isothermal crystallization for the indicated crystallization time at 138°C.

The melting behavior of virgin iPP and β-nucleated iPPs after completing of isothermal crystallization were also investigated by DSC with a heating rate of 10°C/min. The melting traces of (a) iPP, (b) iPP/WBG, and (c) iPP/TMB5 recorded after isothermal crystallization at indicated temperatures, are plotted in Figure 7(a–c), respectively. For all the samples investigated, as mentioned earlier, the melting curves shift to a higher temperature with increasing T_c, which may attribute to the annealing effect during the isothermal crystallization (lamella thickening and crystal perfection degree improving). As shown in Figure 7(a), the melting profile of virgin iPP mainly shows the endotherm referring to α-form, which means almost only α-form appeared in virgin iPP after isothermally crystallized at the whole T_c range adopted in this work. However, for the β-nucleated specimens, as shown in Figure 7(b,c), the melting traces are different with the changes of T_c. Almost only β-form endothermic peak presents on the melting traces of samples crystal-

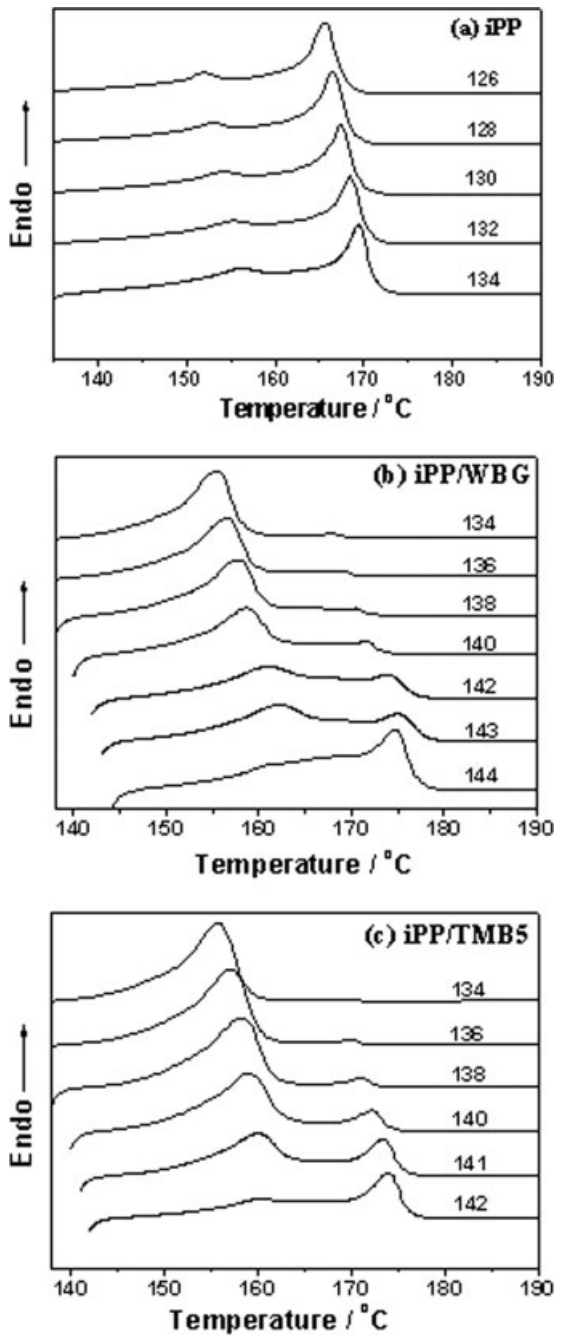

Figure 7 DSC melting traces of (a) iPP, (b) iPP/TMB5, and (c) iPP/WBG after isothermally crystallized at the indicated temperature.

lized at relative lower T_c (134–138°C). With the further increase of the T_c, the endotherm of α-form appears and gradually intensifies, which indicates the more and more α-form developed during the isothermal crystallization process.

A particular growth feature of the β-form is the transformation from metastable β-form into α-form.[9,21,33] Many studies dealt with the kinetic characteristics of growths of iPP contained a certain content of β-form, and these comprehensive investigations revealed that the formation of β-form had an upper and lower (threshold) temperature, $T(\beta\alpha)$ and $T(\alpha\beta)$, respectively.[1,6,21,33–38] The growth rate of α-form exceeds β-form at temperatures below a $T(\alpha\beta)$ and above $T(\beta\alpha)$ while β-form grows faster only between these two temperatures. A further increase in T_c in the range of $T_c > T(\beta\alpha)$ enhances the probability of β-α transitions, which becomes predominant as it approaches the melting temperature of β-form.

It is believed that α-nucleating agents are effective in the whole temperature range below the melting temperature of the α-form, while the β-nucleating agents are active only below $T(\beta\alpha)$.[1] In the present work, when the T_c is 140°C, the dominant modification in both nucleated samples is β-form. However, when T_c increases to 142°C, there is very little β-form in iPP/TMB5 while the relative content of β-form in iPP/WBG exceeds about 70% [approximately estimated following eq. (2)]. Even at T_c up to 143°C, the endotherm on melting traces associated with β-form of iPP/WBG is still larger than that of α-form. The disappearance of β-form endotherm for iPP/TMB5 occurs between 141 and 142°C, while that for iPP/WBG between 143 and 144°C, as shown in Figure 7(b,c). These results suggest that the addition of WBG expanded the upper limit temperature of forming β-modification, and therefore may induce β-form at a more broader T_c range than TMB5.

Avrami and Lauritzen–Hoffman analysis

Generally, the isothermal crystallization kinetics is analyzed by using classical Avrami model, as follows:[39–41]

$$1 - X_t = \exp(-Z_t t^n) \tag{5}$$

$$\ln[-\ln(1 - X_t)] = \ln Z_t + n \ln t \tag{6}$$

Here, X_t is the relative crystallinity determined from eq. (4) at time t; Z_t is the overall crystallization rate constant; n is the Avrami exponent which is relevant to the mechanism of nucleation, and it contains information on nucleation and growth geometry. The parameters Z_t and n could be determined from the plots of $\ln[-\ln(1 - X_t)]$ versus $\ln t$ at different temperatures for the isothermal crystallization, as shown in Figure 8. From eq. (5) we can also determine the half crystallization time $t_{1/2}$ from Z_t and n as $t_{1/2} = (\ln 2/Z_t)^{1/n}$. The calculated $t_{1/2}$ accords very well with the actual $t_{1/2}$ determined from Figure 3. This indicates that the Avrami model is appropriate to analyze the isothermal kinetics of such systems. All these data are listed in Table I.

Figure 9 shows the plots of relative crystallinity versus time for iPP and β-nucleated iPP at 134°C. It is clear that the addition of nucleating agents short-

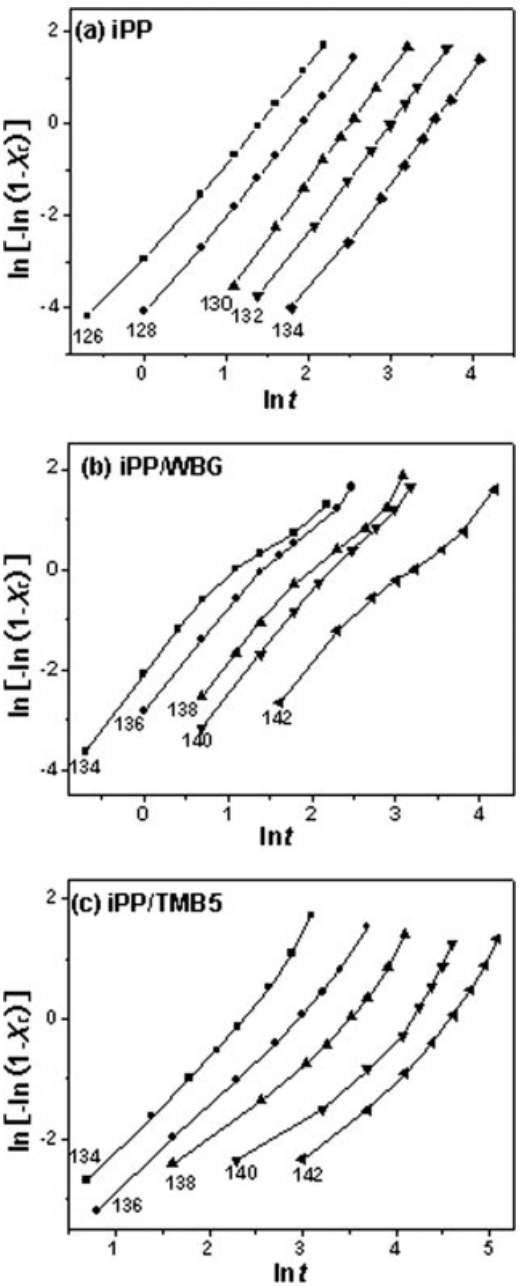

Figure 8 Plots of ln[− ln(1 − X_t)] versus ln t for isothermal crystallization at indicated temperature of (a) iPP, (b) iPP/WBG, and (c) iPP/TMB5, respectively.

ens the crystallization time of iPP considerably. The addition of 0.06 wt % of TMB5 leads to a reduction in the $t_{1/2}$ of about 71% relative to virgin iPP (from 29.6 min to 8.6 min); and 0.08 wt % of WBG cause a larger decrease of $t_{1/2}$ by about 93% shorter than that for virgin iPP (from 29.6 min to 2.2 min). Furthermore, with the addition of these nucleating agents, the overall crystallization rate constant, Z_t, calculated from the Avrami equation, increases sharply from 0.00023 to 0.021 and 0.12 for iPP/TMB5 and iPP/WBG, respectively. On the basis of these results, WBG is a more efficient β-nucleating agent than TMB5 in accelerating the crystallization rate of iPP at the T_c region investigated in this work.

The growth rate of crystallization G can be expressed as follows according to the Lauritzen–Hoffman theory:[41–43]

$$G = G_0 \exp\left(\frac{-U^*}{R(T_c - T_\infty)}\right) \exp\left(\frac{-K_g}{T_c \Delta T_f}\right) \tag{7}$$

where G_0 is a pre-exponential term, U^* is the energy of the transport of the chains in the melt, and the value of U^* is 6270 J/mol for iPP, R is the gas constant, T_c is the crystallization temperature, and T_∞ is the equilibrium melting temperature at which all motion associated with viscous flow ceases and is given by T_g − 30 K (T_g is 263 K for iPP), ΔT is the supercooling temperature, defined as $T_m^0 - T_c$, where T_m^0 is the equilibrium melting temperature (T_m^0 is 481 K for iPP), f is a correcting factor for variation in the heat of fusion with temperature and is defined as $f = 2T_c/(T_m^0 - T_c)$, and K_g is the nucleation constant.

Using the kinetic growth rate constant Z_t and the Avrami exponent n, combined with the half crystallization time ($t_{1/2}$), then we obtain:

$$\ln(t_{1/2})^{-1} + \frac{U^*}{R(T_c - T_\infty)} = A_n - \frac{K_g}{T_c \Delta T_f} \tag{8}$$

Thus, the plot of $\ln(t_{1/2})^{-1} + U^*/R(T_c - T_\infty)$ versus $1/(T_c \Delta T_f)$ will give a straight line as shown from Figure 10. The nucleation constant K_g can be determined from the slope of the line, and the results are listed in Table I.

The fold surface free energy σ_e can be obtained by the following equation:

$$K_g = 4\sigma\sigma_e \frac{b_0 T_m^0}{k\Delta H} \tag{9}$$

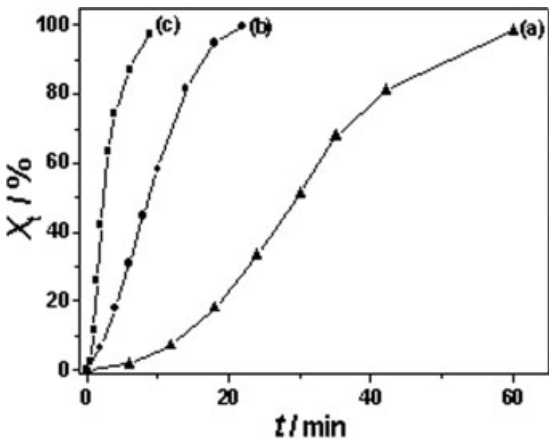

Figure 9 Plots of relative crystallinity versus time at 134°C of (a) iPP, (b) iPP/WBG, and (c) iPP/TMB5, respectively.

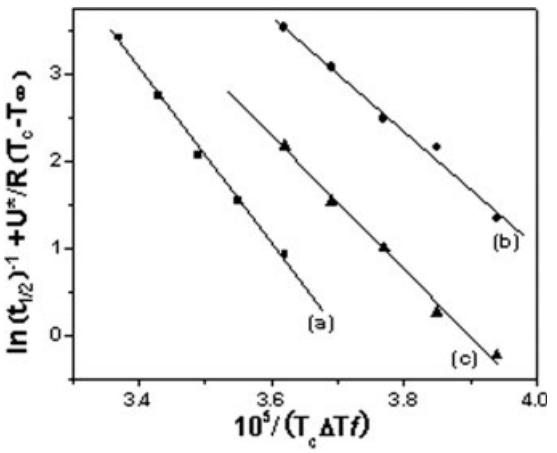

Figure 10 Plots of $\ln(t_{1/2})^{-1} + U^*/R(T_c - T_\infty)$ versus $1/(T_c\Delta T_f)$ for (a) iPP, (b) iPP/WBG, and (c) iPP/TMB5, respectively.

where k is the Boltzman constant, b_0 the thickness of the molecular layer determined by lattice parameters, ΔH is the theoretical heat of fusion, and σ and σ_e are interfacial free energies per unit area parallel and perpendicular to the molecular chain direction, respectively. The value of σ can be obtained from the following expression:

$$\sigma = ab_0\Delta H \tag{10}$$

where a is an empirical constant close to 0.1, b_0 is 6.56×10^{-10} m and ΔH is 1.34×10^8 J/m^3 for iPP; then the value of σ for iPP is 8.79×10^{-3} J/m^2, and so the fold surface free energy σ_e can be calculated from K_g.

K_g and σ_e are also showed in Table I. It indicates that the addition of β-nucleating agents can decrease fold surface free energy obviously, the σ_e of virgin iPP is 0.166 J/m^2, while the value of that is 0.126 J/m^2 and 0.111 J/m^2 for TMB5 and WBG nucleated iPP, respectively. The smaller the fold-free energy of crystallization surface is, the easier the macromolecule chain to form crystal structure. Therefore, the addition of both nucleating agents increases the nucleation and crystallization rate of iPP. The conclusions from Hoffman theory accord very well with the Avrami analysis.

CONCLUSIONS

The crystallization kinetics of virgin iPP and two β-nucleated iPP systems based on WBG and TMB5 were investigated in isothermal conditions. The addition of these nucleating agents induced almost pure β-form in nucleated samples, along with a considerable increase in the $T_{c-\text{onset}}$ was observed. Kinetic parameters obtained from Avrami equation indicated that both agents increased the crystallization rate and shortened the crystallization time of iPP significantly. The Lauritzen–Hoffman theory analysis also revealed that the WBG was more effective not only in increasing the nucleus number, but also in accelerating the growth rate of crystallization: the nucleation constant (K_g) is 6.64×10^5 K^2 for iPP/WBG and 7.58×10^5 K^2 for iPP/TMB5, and the surface free energy of the developing crystals (σ_e) is 0.111 J/m^2 and 0.126 J/m^2, respectively. For the nucleated samples, the melting curves shift to higher temperatures and the endotherm corresponding to α-form gradually aggrandizes with the increase of T_c, which indicates that more of α-form has been developed at the expense of β-form. The decline in the content of β-form when nucleated samples isothermally crystallize at high temperatures could be ascribed to a transformation from β-form into α-form. The disappearance of β-form endotherm for iPP/TMB5 occurrs between 141 and 142°C, while that for iPP/WBG between 143 and 144°C. WBG was more effective than TMB5 in delaying this transformation.

References

1. Varga, J. In Polypropylene, Structure, Blends, and Composites; Karger-Kocsis, J., Ed.; Chapman & Hall: London, 1995; Vol. 1, p 56.
2. Garbarczyk, J.; Paukszta, D. Colloid Polym Sci 1985, 263, 985.
3. Shi, G.; Huang, B.; Zhang, J. Makromol Chem Rapid Commun 1984, 5, 573.
4. Ikeda, N.; Yoshimura, M.; Mizoguchi, K.; Kitagawa, H.; Kawashima, Y.; Sadamitsu, K.; Kawahara, Y. Eur. Pat. 557,721 (1993).
5. Mohmeyer, N.; Schmidt, H.-W.; Kristiansen, P. M.; Altstadt, V. Macromolecules 2006, 39, 5760.
6. Varga, J.; Menyhard, A. Macromolecules 2007, 40, 2422.
7. Tordjeman, Ph.; Robert, C.; Marin, G.; Gerard, P. Eur Phys J E 2001, 4, 459.
8. Chen, H. B.; Karger-Kocsis, J.; Wu, J. S.; Varga, J. Polymer 2002, 43, 6505.
9. Varga, J. J Therm Anal 1986, 31, 165.
10. Varga, J. J Therm Anal 1989, 35, 1891.
11. Varga, J.; Ehrenstein, G. W. Polymer 1996, 37, 5959.
12. Marco, C.; Gómez, M. A.; Ellis, G.; Arribas, J. M. J Appl Polym Sci 2002, 86, 531.
13. Lovinger, A.; Chua, J.; Gryte, C. J Polym Sci Polym Phys Ed 1977, 15, 641.
14. Pawlak, A.; Piorkowska, E. Colloid Polym Sci 2001, 279, 939.
15. Zipper, P.; Janosi, A.; Wrentschur, E.; Abuja, P. M.; Knabl, C. Prog Colloid Polym Sci 1993, 93, 377.
16. Varga, J; Karger-Kocsis, J. J Polym Sci Part B: Polym Phys 1996, 34, 657.
17. Grein, C. Adv Polym Sci 2005, 188, 43.
18. Feng, J. C.; Chen, M. C.; Huang, Z. T.; Guo, Y. Q.; Hu, H. Q. J Appl Polym Sci 2002, 85, 1742.
19. Feng, J. C.; Chen, M. C. Polym Int 2003, 52, 42.
20. Vychopnová, J.; Habrová, V.; Obadal, M.; Cermák, R.; Cabla, R. J Therm Anal 2006, 86, 687.
21. Lotz, B. Polymer 1998, 39, 4561.
22. Turner-Jones, A.; Aizlewood, J. M.; Beckett, D. R. Makromol Chem 1964, 75, 134.

23. Grein, C.; Plummer, C. J. G.; Kausch, H. H.; Germain, Y.; Beguelin, P. Polymer 2002, 41, 3279.
24. Li, J. X.; Cheung, W. L.; Jia, D. Polymer 1999, 40, 1219.
25. Li, J. X.; Cheung, W. L. Polymer 1998, 39, 6935.
26. Shangguan, Y. G.; Song, Y. H.; Peng, M.; Li, B. P.; Zheng, Q. Eur Polym J 2005, 41, 1766.
27. Gahleitner, M.; Wolfschwenger, J.; Bachner, C; Bernreitner, K; Neißl, W. J Appl Polym Sci 1996, 61, 649.
28. Fillon, B.; Lotz, B.; Thierry, A.; Wittmann, J. C. J Polym Sci Part B: Polym Phys Ed 1993, 31, 1395.
29. Sterzynski, T.; Øysæd, H. Polym Eng Sci 2002, 44, 352.
30. Wang, K. F.; Mai, K. C.; Zeng, H. M. J Appl Polym Sci 2002, 78, 2547.
31. Kim, C. Y.; Kim, Y. C.; Kim, S. C. Polym Eng Sci 1993, 33, 1445.
32. Menyhard, A.; Varga, J.; Molnar, G. J Therm Anal 2006, 83, 625.
33. Yuan, Q.; Jiang, W.; An, L. J Colloid Polym Sci 2004, 282, 1236.
34. Varga, J. J Macromol Sci Phys 2002, 41, 1121.
35. Padden, F. J.; Keith, H. D. J Appl Phys 1959, 30, 1749.
36. Varga, J.; Mudra, I.; Ehrenstein, G. W. J Appl Polym Sci 1999, 74, 2357.
37. Varga, J. Angew Makromol Chem 1982, 104, 79.
38. Varga, J. J Mater Sci 1992, 27, 2557.
39. Avrami, M. J Chem Phys 1939, 7, 1103.
40. Avrami, M. J Chem Phys 1940, 8, 212.
41. Lim, G. B. A.; Lloyd, D. R. Polym Eng Sci 1993, 33, 529.
42. Hoffman, J. D. Polymer 1983, 24, 26.
43. Zhu, G.; Li, C. C.; Li, Z. Y. Eur Polym J 2001, 37, 1007.